Ceramics International xxx (xxxx) xxx–xxx

Contents lists available at ScienceDirect

Ceramics International

journal homepage: www.elsevier.com/locate/ceramint

Variation in structures and photoluminescence spectra of $Ba_xEu_{1-x}Al_2O_4$ powders

Min-Ho Lee[a], Bong-Ki Min[b], Woo-Sik Jung[a,*]

[a] School of Chemical Engineering, College of Engineering, Yeungnam University, 280 Daehak-ro, Gyongsan 38541, Republic of Korea
[b] Center for Research Facilities, Yeungnam University, 280 Daehak-ro, Gyongsan 38541, Republic of Korea

ARTICLE INFO

Keywords:
Barium europium aluminate
IR
Raman
Rietveld method
SAED
Photoluminescence

ABSTRACT

Barium europium(II) aluminate ($Ba_xEu_{1-x}Al_2O_4$) powders were prepared by a solid-state reaction among barium carbonate ($BaCO_3$), europium oxide (Eu_2O_3), and alumina (Al_2O_3) powders at 1400 °C for 3 h under a mixed gas flow of H_2 and N_2. The powders were characterized by powder X-ray diffraction (XRD), infrared and Raman spectroscopy, and photoluminescence (PL). With increasing Ba^{2+} content in $Ba_xEu_{1-x}Al_2O_4$, the structure of $Ba_xEu_{1-x}Al_2O_4$ changed from a monoclinic ($P2_1$) to hexagonal ($P6_3$) phase. The hexagonal ($P6_322$) phase was also observed between the two phases. The XRD pattern of a single $Ba_{0.6}Eu_{0.4}Al_2O_4$ phase, which has not been reported in the literature, was refined by the Rietveld method and its structure was confirmed by selected-area electron diffraction. With increasing x value, the emission peak in the PL spectra of $Ba_xEu_{1-x}Al_2O_4$ became weaker (x = 0–0.4) and then more intense (x = 0.6–0.98), and its position showed a blue shift from 520 to 498 nm.

1. Introduction

Strontium aluminate ($SrAl_2O_4$) and barium aluminate ($BaAl_2O_4$) with a tetrahedral AlO_4 framework structure have attracted considerable interest as the host materials of phosphors for long afterglow luminescence [1–12]. Eu^{2+}-doped phosphors exhibit broad emission bands after excitation, due to electron transition from the $4f^65d^1$ excited states into the $4f^7$ ground states. The wavelength and intensity of the corresponding emission are influenced strongly by the host lattice. Most of Eu^{2+}-doped $SrAl_2O_4$ ($SrAl_2O_4$:Eu^{2+}) phosphors with green emission (ca. 520 nm) have a monoclinic ($P2_1$ space group) structure [1,3–8]. Recently, Shinozaki et al. prepared a hexagonal ($P6_322$)-$SrAl_2O_4$:Eu^{2+} phosphor and reported that the photoluminescence was more intense for the hexagonal structure than for the monoclinic one [8]. On the other hand, Eu^{2+}-doped $BaAl_2O_4$ ($BaAl_2O_4$:Eu^{2+}) with a hexagonal structure ($P6_322$ and $P6_3$ space groups) has a bluish-green emission peak (at ca. 490 nm) [2,3,9–11]. Chen et al. showed that the structure of $Ba_xSr_{1-x}Al_2O_4$:Eu^{2+} phosphors underwent a monoclinic to hexagonal phase transformation at $x \geq 0.3$ and their emission peak was blue-shifted (520.5–502.2 nm) from x = 0–1 [12].

In this study, $Ba_xEu_{1-x}Al_2O_4$ powders were obtained by a solid-state reaction among $BaCO_3$, Eu_2O_3, and Al_2O_3 powders at 1400 °C for 3 h under a mixed gas flow of H_2 and N_2, and the change in their structure with x was investigated by powder X-ray diffraction (XRD), infrared (IR) spectroscopy, and Raman spectroscopy. The XRD pattern of a single $Ba_{0.6}Eu_{0.4}Al_2O_4$ phase, which has not been reported in the literature, was refined by the Rietveld method and its selected-area electron diffraction (SAED) pattern was measured. The photoluminescence (PL) spectra of the $Ba_xEu_{1-x}Al_2O_4$ phosphors were measured and compared with those of $Ba_xSr_{1-x}Al_2O_4$:Eu^{2+}. Note that the crystal radius of Eu^{2+} (131 pm for CN = 6) is close to that of Sr^{2+} (132 pm for CN = 6) [13].

2. Experimental procedure

The starting materials, $BaCO_3$ (99.0%, Kanto Chemical Co.), Eu_2O_3 (99.9%, Sigma-Aldrich Co.), and δ-Al_2O_3 (CR125, Baikalox International) powders, were used as received.

2.1. Synthesis of $Ba_xEu_{1-x}Al_2O_4$ powders

$Ba_xEu_{1-x}Al_2O_4$ powders were prepared by a solid-state reaction method. The $BaCO_3$, Eu_2O_3, and δ-Al_2O_3 powders at the ratio of the nominal composition were mixed thoroughly in an agate mortar and transferred into an alumina crucible. The crucible was heated to 1400 °C under a mixed gas flow of H_2 (10 vol%) and N_2 (hereafter, 10 vol% H_2/N_2). The gas flow rate was 100 ml/min and the duration was 3 h.

* Corresponding author.
E-mail address: wsjung@yu.ac.kr (W.-S. Jung).

https://doi.org/10.1016/j.ceramint.2017.12.105
Received 26 October 2017; Received in revised form 12 December 2017; Accepted 14 December 2017

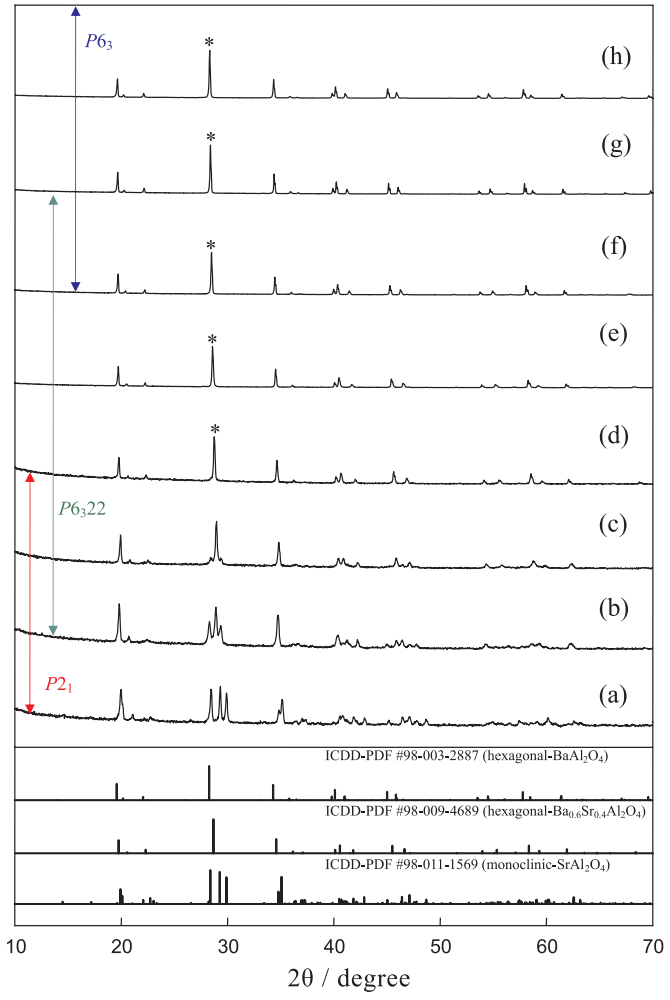

Fig. 1. XRD patterns of $Ba_xEu_{1-x}Al_2O_4$ (x = (a) 0, (b) 0.3, (c) 0.35, (d) 0.4, (e) 0.6, (f) 0.75, (g) 0.9, and (h) 1.0) obtained by calcining mixtures of $BaCO_3$, Eu_2O_3, and δ-Al_2O_3 at 1400 °C for 3 h under a flow of 10 vol% H_2/N_2.

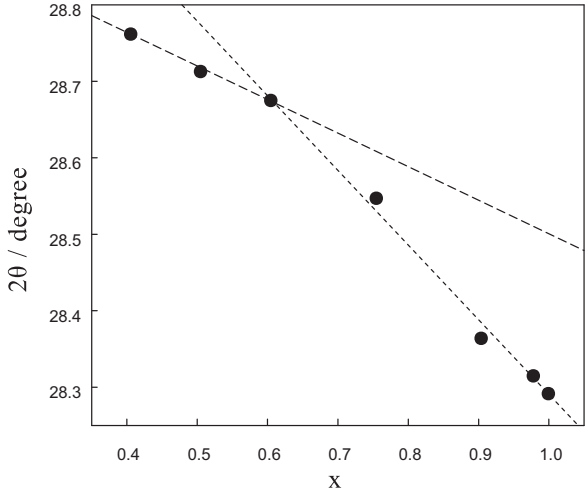

Fig. 2. Plot of the * peak position in Fig. 1 against x value for $Ba_xEu_{1-x}Al_2O_4$.

2.2. Product characterization

The product powders were characterized by powder XRD (PANalytical X'Pert PRO MPD X-ray diffractometer) with Cu-Kα radiation operating at 40 kV and 30 mA, IR spectroscopy (Nicolet 6700, Thermo Scientific), and Raman spectroscopy. The Raman spectra were measured on a Raman microscope (Horiba Jobin Yvon XploRa Plus) with an excitation wavelength of 532 nm using an objective lens with 100x magnification. The morphology was examined by scanning electron microscopy (SEM, Hitachi S-4200). The PL spectra were measured on a JASCO FP-6500 spectrofluorometer with a 150 W xenon lamp. The single phase of $Ba_{0.6}Eu_{0.4}Al_2O_4$ was confirmed by the Rietveld refinement method [14] using X'pert Highscore Plus software [15] and by selected area electron diffraction (SAED) using a transmission electron microscope (TEM, FEI Tecnai F20). All measurements were taken at room temperature.

3. Results and discussion

3.1. Synthesis and characterization of $Ba_xEu_{1-x}Al_2O_4$

$Ba_xEu_{1-x}Al_2O_4$ powders were obtained by calcining mixtures of $BaCO_3$, Eu_2O_3, and δ-Al_2O_3 powders at 1400 °C for 3 h under a flow of 10 vol% H_2/N_2. Fig. 1 presents their XRD patterns. As shown in Fig. 1(a), the sample with x = 0 exhibited peaks assigned to monoclinic (*m*-)$EuAl_2O_4$ with the $P2_1$ space group [16,17]. The previous paper showed that the XRD pattern of *m*-$EuAl_2O_4$ was similar to that of *m*-$SrAl_2O_4$ [17] because of the similarity in crystal radius between Eu^{2+} and Sr^{2+} ions [13]. The XRD pattern (Fig. 1(b)) of the sample with x = 0.3 was slightly different from that of *m*-$EuAl_2O_4$ in terms of the position of all peaks and relative intensity of the three peaks around 29.3°. The shift of the peaks to a lower degree was attributed to the partial substitution of a larger Ba^{2+} ion for Eu^{2+}. The difference indicates that the sample with x = 0.3 contained a new phase, *i.e.*, hexagonal $Ba_{0.6}Eu_{0.4}Al_2O_4$ (see below). With increasing x value, the intensity of the three peaks around 29.3° decreased gradually. The XRD pattern (Fig. 1(e)) of the sample with x = 0.6 was similar to that of hexagonal (*h*-)$Ba_{0.6}Sr_{0.4}Al_2O_4$ (ICDD-PDF #98-009-4689) [18], suggesting that the sample with x = 0.6 was a single hexagonal phase with the $P6_322$ space group. The similarity between the two XRD patterns was attributed to the similar crystal radii of Eu^{2+} and Sr^{2+} ions. When x was larger than 0.6, the position of the peaks was still shifted to a lower degree. As shown in Fig. 1(h), the sample with x = 1 was a single phase of *h*-$BaAl_2O_4$ (ICDD-PDF #98-003-2887) with the $P6_3$ space group. Therefore, the shift in position suggests that the samples with $0.6 < x < 1$ might be a mixture of powders with the $P6_322$ and $P6_3$ space groups. These results showed that there is a structural phase boundary between the monoclinic and hexagonal $Ba_xEu_{1-x}Al_2O_4$ powders. The x value at the boundary can be estimated from a plot of the position of the most intense peak (marked by asterisks) in Fig. 1 against the x value for $Ba_xEu_{1-x}Al_2O_4$. As shown in Fig. 2, the plot was not linear, *i.e.*, two lines crossed at x = 0.6.

The difference in the XRD patterns of $Ba_xEu_{1-x}Al_2O_4$ ($0.6 < x < 1$) between the $P6_322$ and $P6_3$ space groups could not be discerned easily, which was similar to that of $Ba_xSr_{1-x}Al_2O_4$ ($0.6 < x < 1$) [19]. The IR and Raman spectra were also measured to monitor the phase transition from the monoclinic to hexagonal structure in $Ba_xEu_{1-x}Al_2O_4$ with increasing x value. Fig. 3(A) shows the IR spectra assigned to vibrations of AlO_4 groups in $Ba_xEu_{1-x}Al_2O_4$. The tetrahedral (T_d) AlO_4 group has nine normal modes, *i.e.*, symmetric stretching (ν_1), doubly degenerate symmetric bending (ν_2), triply degenerate antisymmetric stretching (ν_3) and triply degenerate antisymmetric bending (ν_4), in which all four vibrations are Raman active, whereas only ν_3 and ν_4 vibrations are IR active [20]. All AlO_4 groups in $Ba_xEu_{1-x}Al_2O_4$ were distorted from T_d symmetry, leading to the removal of the degeneracy of vibrations and an increase in the number of IR-active vibrations. The crystal structures (Fig. 4) and point groups (Table 1) of the Al^{3+} sites for *m*($P2_1$)-$EuAl_2O_4$, *h*($P6_322$)-$Ba_{0.6}Eu_{0.4}Al_2O_4$, and *h*($P6_322$, $P6_3$)-$BaAl_2O_4$ were obtained by using CrystalMaker software [21]. According to Table 1, all AlO_4 groups in *m*-$EuAl_2O_4$ have C_1 symmetry, whereas those in *h*($P6_322$)-$Ba_{0.6}Eu_{0.4}Al_2O_4$ and *h*($P6_322$)-$BaAl_2O_4$ have C_3 symmetry. The number